JOURNAL OF CATALYSIS **176,** 321–328 (1998)
ARTICLE NO. CA982061

Studies of Decomposition of H_2O_2 over Manganese Oxide Octahedral Molecular Sieve Materials

H. Zhou,* Y. F. Shen,*,† J. Y. Wang,* X. Chen,* Chi-Lin O'Young,‡ and Steven L. Suib*,§,[1]

*Department of Chemistry, University of Connecticut, Storrs, Connecticut 06269-4060; †Gillette Company, North Atlantic Group, One Gillette Park, Boston, Massachusetts 02127-1096; ‡Texaco Research Center, Texaco Inc. P.O. Box 509, Beacon, New York 12508; and §Department of Chemical Engineering and Institute of Materials Science, University of Connecticut, Storrs, Connecticut 06269

Received September 2, 1997; revised December 11, 1997; accepted February 26, 1998

A series of manganese oxide molecular sieve (OMS) materials has been successfully synthesized. Doping some divalent cations and first row transition metal ions such as Mg^{2+}, Ni^{2+}, Cu^{2+}, Co^{2+}, and Fe^{3+} into the framework of OMS materials to form [M]-OMS materials was also done. The catalytic activities of [M]-OMS materials and commercial MnO_2 for H_2O_2 decomposition were studied. The experimental results show an activity order sequence as follows: most of [M]-OMS materials > commercial MnO_2; [M]-OMS-2 > [M]-OMS-1; and among [M]-OMS-2 samples, [Ni]-OMS-2 > [Cu]-OMS-2 > [Fe]-OMS-2 > [Co]-OMS-2 > [Mg]-OMS-2. The kinetics and a mechanism of H_2O_2 catalytic decomposition over [M]-OMS materials were studied and proposed, as well.

I. INTRODUCTION

H_2O_2 decomposition has been extensively studied (1–14). There are two major reasons why H_2O_2 decomposition is so interesting: (1) H_2O_2 decomposition is a useful model reaction for studying catalytic activity of different materials (2); (2) H_2O_2 might be an efficient oxygen source, if highly active and selective catalysts are available for H_2O_2 decomposition (4). In the past decade, several catalysts have been tested for H_2O_2 decomposition that can be classified into two categories, i.e.: (a) homogeneous and (b) heterogeneous catalysts.

Most homogeneous catalysts are transition metal ion complexes (9), and heterogeneous catalysts are oxides of some transition metals (8). For both homogeneous and heterogeneous catalysts, transition metals play a very important role, since catalytic activity varies with different transition metals doped in the catalysts. This research was focused on the heterogeneous decomposition of H_2O_2 with [M]-OMS catalysts.

Considerable attention has been paid to both catalysts and mechanisms in the area of heterogeneous catalysis for H_2O_2 decomposition (1–14). Generally, certain catalysts have unique physicochemical properties that determine reaction pathways as well as the mechanism of a given reaction. The physicochemical properties of the catalysts, which are very important in heterogeneous catalysis, include oxidation–reduction potential, electronic configuration, coordination numbers, geometry, crystal type, surface area, and particle size as well. However, these properties not only depend on choice of starting materials and chemical compositions for making catalysts, but also they can be varied by various preparation methods. Since the choices of catalysts for H_2O_2 decomposition have been limited due to the high cost of catalysts such as silver oxide, platinum, and palladium black, as well as the poor reactivity of some cheaper catalysts such as commercial MnO_2, Co_2O_3, Fe_2O_3, seeking cheaper and more efficient catalysts is significant for H_2O_2 decomposition.

Two basic approaches have been used to look for better catalysts for H_2O_2 decomposition in the past decade. The first involves studying different crystal structures of catalysts with the same chemical composition, e.g., MnO_2. The second approach concerns the study of systems with a mixture of more than two different metal oxides, e.g., MCo_2O_4 (M = Mn, Fe, Cu, Ni, and Zn). Previous studies show that H_2O_2 decomposition over different catalysts may not have the same reaction pathway, however, H_2O_2 decomposition might likely be a first-order reaction (1–14).

Adsorption plays an important role in the field of heterogeneous catalysis. There are several well-known adsorption models widely applied to study mechanisms for most heterogeneous catalytic reactions, which include Langmuir adsorption isotherms, Freundlich adsorption isotherms, and Temkin adsorption isotherms. Among these models, the Langmuir adsorption isotherms have the greatest general utility in application to heterogeneous catalysis because of its simplicity and suitability for both chemical and physical adsorption. In addition, the Langmuir model for adsorption also serves as a starting point in formulating many kinetic expressions and mechanistic studies for many catalyzed reactions.

[1] Author to whom correspondence should be addressed.

0021-9517/98 $25.00

In this research, commercial MnO_2 and synthetic octahedral molecular sieve (OMS) materials were investigated as catalysts in H_2O_2 decomposition. A mechanism for H_2O_2 decomposition was postulated based on the Langmuir–Hinshelwood kinetic model. Other characterization studies of these catalysts were also done.

II. EXPERIMENTAL SECTION

A. Reagents

All reagents were of analytical grade, unless otherwise noted. Distilled deionized water (DDW) was used to prepare materials. H_2O_2 was obtained from J. T. Baker, Inc. The water used to dilute aqueous H_2O_2 was DDW. The total concentration of H_2O_2 was determined by titration with a 0.1 *N* solution of $KMnO_4$.

B. Catalysts

The catalysts were [M]-OMS-1 and [M]-OMS-2 type materials. [M] stands for metals other than manganese doped into the framework of OMS materials. The [M]-OMS-1 materials were synthesized hydrothermally in autoclaves (15). The [M]-OMS-2 samples were synthesized by refluxing and precipitation methods (16). [Ni]-OMS-2(1) and [Ni]-OMS-2(2) were prepared by adding different amounts of corresponding metal nitrate. The commercial MnO_2 was obtained from the Aldrich Chemical Co.

C. Surface Area Measurements

The surface areas of both [M]-OMS-1 and [M]-OMS-2 materials were determined by Brunauer–Emmett–Teller measurements (BET) using nitrogen gas and a multipoint method. The surface areas of [M]-OMS-1 materials range from 140 to 180 m^2/g, and 100 to 120 m^2/g for [M]-OMS-2 materials. The surface area of the commercial MnO_2 is 50–65 m^2/g which was provided by the Aldrich Chemical Co., Milwaukee, WI, U.S.A.

D. X-Ray Powder Diffraction Studies

Both [M]-OMS-1 and [M]-OMS-2 materials were characterized with X-ray powder diffraction (XRD) methods. Data were collected with a Scintag 2000 PDS with Cu Kα X-ray radiation, a beam voltage of 45 kV, and 40 mA beam current.

E. Apparatus and Procedures

The apparatus used for catalytic studies is shown in Fig. 1. A catalyst was loaded into an Erlenmeyer flask. The inlet of the flask was covered by a septum, while the outlet was connected with a metal tube to one end of a U-type glass jar filled with water. The other end of the U-type glass jar was connected to a graduated cylinder by a plastic tube. When the reaction took place, the evolved gaseous oxygen forced water out of the U-type glass jar into the graduated cylinder. During the reaction, the H_2O_2 concentration remaining in the Erlenmeyer flask versus time can be calculated according to the initial concentration of H_2O_2 in the flask and the number of moles of O_2 evolved.

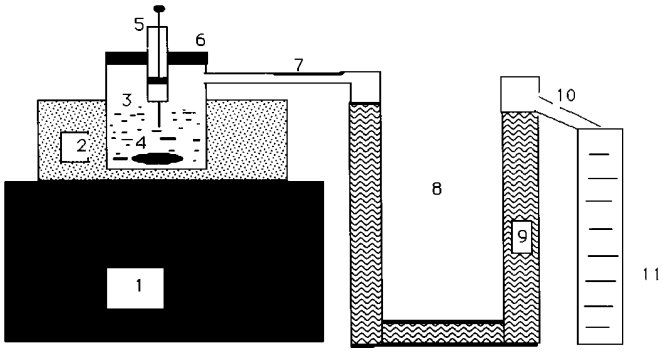

FIG. 1. Experimental apparatus for catalytic decomposition of H_2O_2. 1, magnetic stirring plate; 2, ice bath; 3, flask; 4, magnetic stirring bar; 5, septum; 6, syringe; 7, metal tubing; 8, U-type glass jar; 9, water; 10, plastic tubing; 11, graduated cylinder.

A 20.0 mL solution of H_2O_2 was injected into the flask with 20 mg of a catalyst, and time responses were observed. The H_2O_2 aqueous solution was stirred with a magnetic stirring bar. The volume of water forced out of the flask was measured as a function of time. The concentration of H_2O_2 at any time ($[H_2O_2]_t$) in the reactor can be calculated with the following equations:

$$H_2O_2 \rightarrow 0.5O_2 + H_2O \quad [1]$$

$$[H_2O_2]_t = [H_2O_2]_o - (2n/V), \quad [2]$$

where $[H_2O_2]_o$ is the initial concentration of H_2O_2, and n represents the number of moles of O_2 released from H_2O_2 at time t, which is readily calculated from the ideal gas law, and V is the initial volume of H_2O_2 (20.0 mL). Plots of $[H_2O_2]_t$ versus time (t) were obtained in this manner. The hydrostatic pressure generated in the U-type glass apparatus during reaction was taken into account when the volume of evolved oxygen was determined.

The catalysts studied here include [Co]-OMS-1, [Cu]-OMS-1, [Fe]-OMS-1, [Mg]-OMS-1, [Ni]-OMS-1, [Co]-OMS-2, [Cu]-OMS-2, [Fe]-OMS-2, [Mg]-OMS-2, [Ni]-OMS-2, and commercial MnO_2, where M represents cations which are Co, Cu, Fe, Mg, or Ni ions in the framework of [M]-OMS materials.

III. RESULTS

A. Catalysis Results

The activities of all materials were normalized by their surface areas in the H_2O_2 decomposition. Control experiments were done with no catalysts, and negligible rates of H_2O_2 decomposition were observed.

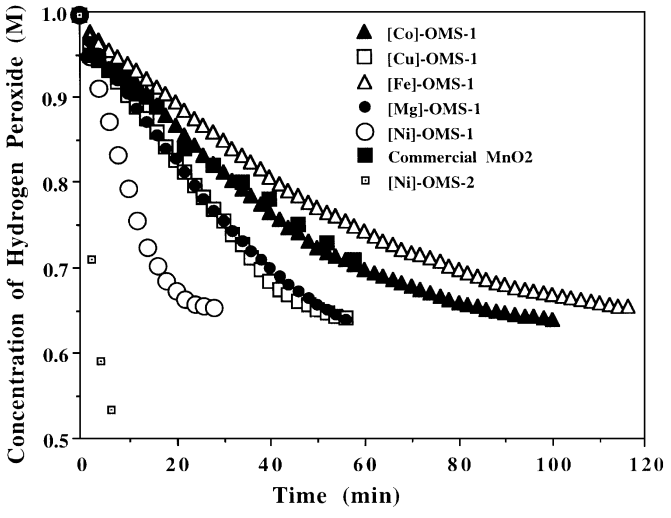

FIG. 2. Comparison of catalytic decomposition of H_2O_2 over [M]-OMS and commercial MnO_2 catalysts at 273 K.

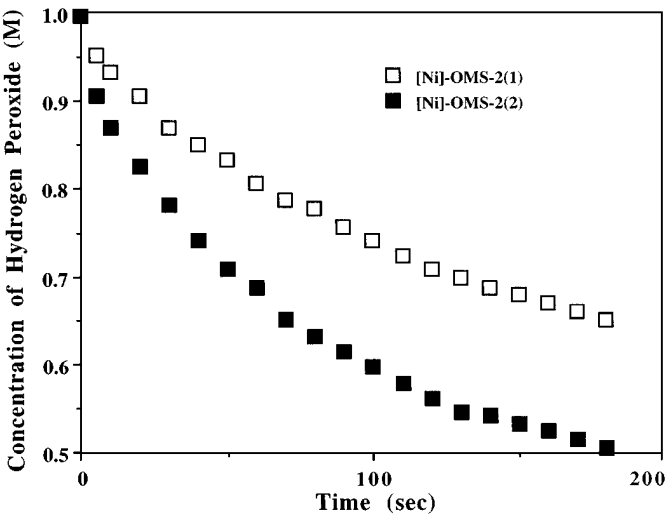

FIG. 4. Comparison of catalytic decomposition of H_2O_2 over different [Ni]-OMS-2 catalysts at 273 K.

Figure 2 shows catalytic activities of [M]-OMS-1, [Ni]-OMS-2, and commercial MnO_2 catalysts at 273 K. The rate of H_2O_2 decomposition with [Ni]-OMS-2 is the fastest of all these catalysts. The order of decreasing rate of H_2O_2 decomposition for these catalysts is [Ni]-OMS-2 > [Ni]-OMS-1 > [Cu]-OMS-1 > [Mg]-OMS-1 > [Co]-OMS-1 > commercial MnO_2 > [Fe]-OMS-1.

Figure 3 shows catalytic activities of different [M]-OMS-2 catalysts for H_2O_2 decomposition at 273 K. The rate of H_2O_2 decomposition with [Ni]-OMS-2 was faster than all other materials. The order of decreasing rate of H_2O_2 decomposition for these catalysts is [Ni]-OMS-2 > [Cu]-OMS-2 > [Mg]-OMS-2 > [Fe]-OMS-2 > [Co]-OMS-2.

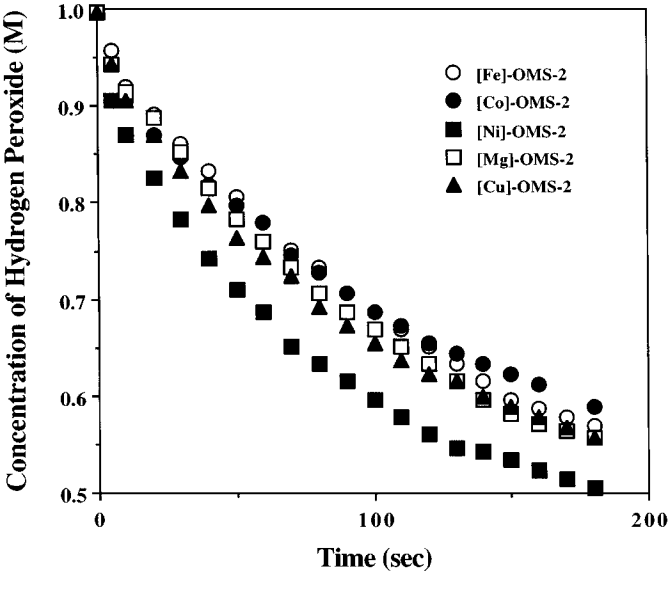

FIG. 3. Comparison of catalytic decomposition of H_2O_2 over [M]-OMS-2 catalysts at 273 K.

Previous studies from our laboratory show that the capacities of OMS-2 materials for accommodating different first row transition metals are different, and for [Ni]-OMS-2 materials the molar ratio of Mn/Ni can be varied over a large range from 196/1 to 59/1 (16). This ratio can be expanded down to about 40/1. In order to investigate the quantitative effect of transition metal dopants versus activities of OMS materials, two [Ni]-OMS-2 materials with different Ni dopants in amount were tested for H_2O_2 decomposition. Figure 4 shows the catalytic activities of [Ni]-OMS-2(1) and [Ni]-OMS-2(2) samples for H_2O_2 decomposition at 273 K whose molar ratios of Mn/Ni are 53 : 1 and 43 : 1, respectively. The rate of H_2O_2 decomposition with [Ni]-OMS-2(2) was faster than [Ni]-OMS-2(1).

B. Stability Studies

The stabilities of [M]-OMS catalysts were also tested. All the catalysts except [Fe]-OMS-1 retained their structures after reaction. Figure 5 shows X-ray diffraction data for [Ni]-OMS-2 catalyst with one of the examples retaining their structures after reaction. However, as shown in Fig. 6, the structure of [Fe]-OMS-1 was changed to the structure of birnessite (16) after H_2O_2 decomposition.

C. Kinetic Studies

The Langmuir–Hinshelwood kinetic model was applied to study the kinetics and the mechanism of H_2O_2 decomposition over only [M]-OMS-2 catalysts, since H_2O_2 decomposition rate over [M]-OMS-2 materials is much faster than others. The used catalysts were collected after reaction (3 h) and retested for H_2O_2 decomposition. No decrease in activity was observed.

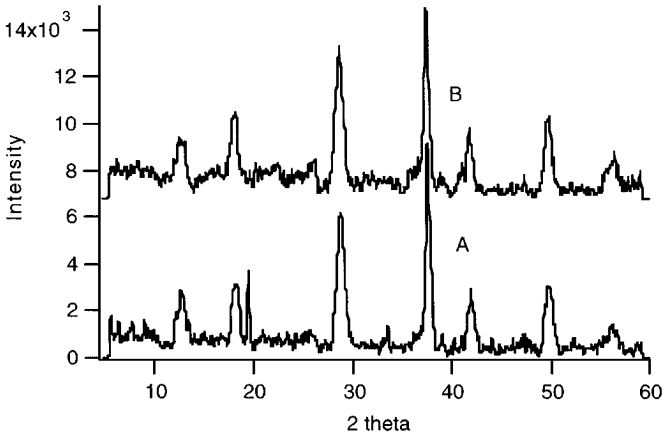

FIG. 5. X-ray diffraction data for [Ni]-OMS-2 catalyst before and after decomposition of H_2O_2 273 K. A, [Ni]-OMS-2 after decomposition of H_2O_2; B, [Ni]-OMS-2 before decomposition of H_2O_2; the Y axis scales for A and B are the same.

The Langmuir–Hinshelwood kinetic model is

$$-r_{H_2O_2} = k_{H_2O_2} \times \frac{K_{H_2O_2}[H_2O_2]_{(aq)}}{1 + K_{H_2O_2}[H_2O_2]_{(aq)}}. \qquad [3]$$

In Eq. [3], $r_{H_2O_2}$ is the rate of H_2O_2 decomposition on the surface of [M]-OMS-2 catalyst, $k_{H_2O_2}$ is the overall rate constant and is independent of the H_2O_2 concentration. $K_{H_2O_2}$ is the adsorption coefficient. Eventually, Eq. [3] can be rewritten as Eq. [4]

$$-\frac{1}{r_{H_2O_2}} = \frac{1}{k_{H_2O_2}} + \frac{1}{k_{H_2O_2} \times K_{H_2O_2}} \times \frac{1}{[H_2O_2]_{(aq)}}. \qquad [4]$$

In Eq. [4], we are assuming

$$y = -\frac{1}{r_{H_2O_2}}, \quad x = \frac{1}{[H_2O_2]_{(aq)}}.$$

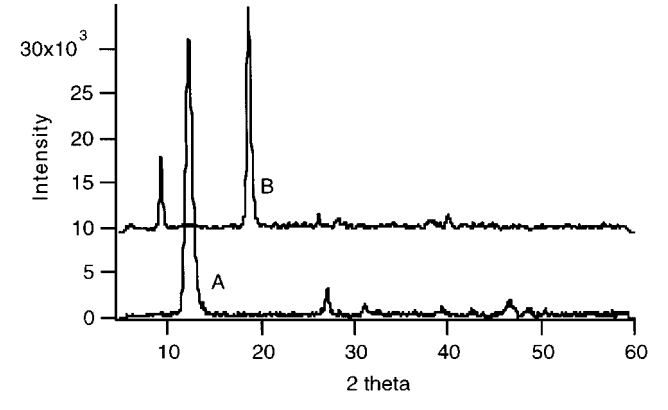

FIG. 6. X-ray diffraction data for [Fe]-OMS-1 catalyst before and after decomposition of H_2O_2 273 K. A, [Fe]-OMS-1 after decomposition of H_2O_2; B, [Fe]-OMS-1 before decomposition of H_2O_2; the Y axis scales for A and B are the same.

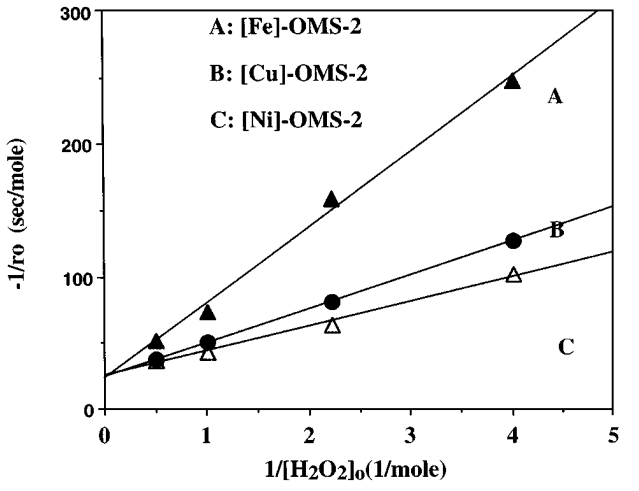

FIG. 7. Kinetic plots of catalytic decomposition of H_2O_2 over [M]-OMS-2 catalysts.

A plot of y versus x can be drawn. Therefore, two parameters ($k_{H_2O_2}$ and $K_{H_2O_2}$) in Eq. [4] can be determined. In these plots, the initial rate ($\mathbf{r}_o$) and the initial concentration of H_2O_2 ($[H_2O_2]_o$) should be used. It is theoretically expected that larger values of both $k_{H_2O_2}$ and $K_{H_2O_2}$ correspond to faster decomposition rates.

Kinetic studies were carried out by using two sets of [M]-OMS materials with four different H_2O_2 concentrations (1.990 M, 0.997 M, 0.449 M and 0.249 M) at 273 K. One includes [Cu]-OMS-2, [Fe]-OMS-2, and [Ni]-OMS-2 catalysts, while another includes [Ni]-OMS-2(1) and [Ni]-OMS-2(2) catalysts. Figures 7 and 8 are plots of reciprocals of initial rates ($\mathbf{r}_o$) of H_2O_2 decomposition versus reciprocals of initial concentrations of H_2O_2 ($[\mathbf{H_2O_2}]_o$) for two sets of catalysts, respectively. Apparently a good linear relationship is revealed in both plots.

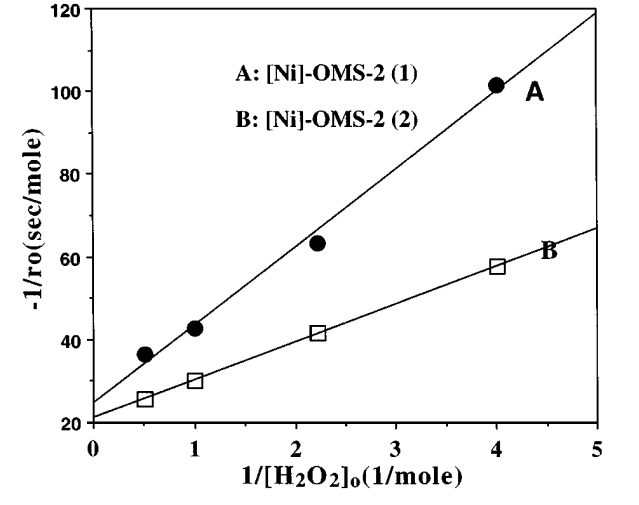

FIG. 8. Kinetic plots of catalytic decomposition of H_2O_2 over [Ni]-OMS-2(1) and [Ni]-OMS-2(2) catalysts.

TABLE 1

Kinetic Parameters of Langmuir–Hinshelwood Kinetic Model for Decomposition of H_2O_2 over [M]-OMS Catalysts

Catalyst	$k_{H_2O_2}(M \cdot Min^{-1})$	$K_{H_2O_2}(M^{-1})$
[Cu]-OMS-2	0.041	0.952
[Fe]-OMS-2	0.044	0.399
[Ni]-OMS-2(1)	0.041	1.318
[Ni]-OMS-2(2)	0.047	2.300

Two important parameters, the rate constant and the adsorption coefficient determined from the Langmuir–Hinshelwood kinetic model for H_2O_2 decomposition over [M]-OMS-2 are shown in Table 1. The increasing order of magnitude in $\boldsymbol{k_{H_2O_2}}$ is [Ni]-OMS-2 (2) > [Fe]-OMS-2 > [Ni]-OMS-2 = [Cu]-OMS-2, and the increasing order of magnitude in $\boldsymbol{K_{H_2O_2}}$ is [Ni]-OMS-2 (2) > [Ni]-OMS-2 (1) > [Cu]-OMS-2 > [Fe]-OMS-2.

After catalytic H_2O_2 decomposition, the supernatants of the product solutions were separated by centrifugation, and also analyzed by ICP-atomic absorption spectroscopy (AAS). These results are shown in Table 2. Table 2 shows that the supernatants contain four types of cations, which are K^+, Mn^{2+}, Mg^{2+}, and the corresponding transition metal dopants, respectively. The ICP-AAS data show that the concentrations of these cations vary from one sample to another.

IV. DISCUSSION

A. Catalytic Results

The data shown in Figs. 2, 3, and 4 suggest that most [M]-OMS materials give a higher activity than commercial MnO_2 for H_2O_2 decomposition. The activity of [M]-OMS-2 is even higher than [M]-OMS-1. The activity of different [M]-OMS materials for H_2O_2 decomposition varies from one to another. Ni dopants significantly increase the catalytic activity of both [M]-OMS-1 and [M]-OMS-2 materials for H_2O_2 decomposition.

TABLE 2

Concentrations of Metal Ions Released from [M]-OMS Catalysts and Commercial MnO_2 in Supernatant Solutions after Decomposition of H_2O_2

Supernatant	Concentration of metal ions (mg/L)						
	K	Mn	Co	Cu	Fe	Mg	Ni
[Co]-OMS-1	5545	945	21			60	
[Cu]-OMS-1	357	2787		7		9952	
[Fe]-OMS-1	3323	429			91	8122	
[Mg]-OMS-1	461	66				6825	
[Ni]-OMS-1	411	109				10297	13
[Co]-OMS-2	3205	1612	530			45	
[Cu]-OMS-2	4234	426		8		12	
[Fe]-OMS-2	2930	1380			44	26	
[Mg]-OMS-2	6676	1335				433	
[Ni]-OMS-2	5286	1459				31	63
Commercial MnO_2		8636				84	

Comparing [M]-OMS materials to commercial MnO_2, first of all, they are different in chemical composition. [M]-OMS materials contain some other transition metal cations that may sit in the framework or inside of the tunnels of [M]-OMS materials, while commercial manganese dioxide does not. According to our results, doping different transition metal cations into [M]-OMS materials may significantly influence their physicochemical properties such as chemical compositions, oxidation state, acidity or basicity, type and concentration of active sites, etc., and the increase of Lewis acid sites in [M]-OMS materials with respect to OMS materials may result from the transition metal dopants (15–16).

Second, [M]-OMS materials have a greater surface area than commercial MnO_2. Data based on the normalized surface area in Fig. 2 show that most [M]-OMS materials have a faster H_2O_2 decomposition rate than commercial MnO_2. Higher activity of [M]-OMS materials toward H_2O_2 decomposition may be due to their transition metal dopants, instead of their relatively high surface areas.

Two important properties of OMS materials are pore size and surface area. The tunnel sizes of [M]-OMS-1 and [M]-OMS-2 materials are 6.9 and 4.6 Å, respectively. The surface areas of [M]-OMS-1 materials studied here are between 140 to 180 m^2/g, and the surface areas of [M]-OMS-2 materials reported here are between 100 to 120 m^2/g. Since there is no significant difference between the two materials in surface area, therefore, the data in Fig. 2 may once again suggest that there is little influence of surface areas of the various [M]-OMS catalysts in H_2O_2 decomposition. However, the faster rate of H_2O_2 decomposition over [M]-OMS-2 materials may be rather simply attributed to the fact that the size of the tunnel in [M]-OMS-2 is closer to the size of H_2O_2 which may provide shape selective effects (16, 19).

The observation showing that different transition metals in [M]-OMS materials vary their activities for H_2O_2 decomposition implies that framework transition metal dopants into both [M]-OMS-1 and [M]-OMS-2 materials function in a similar way. One of the reasons for this observation probably can be explained by their similarities which include MnO_6 structural units existing in both materials, and transition metal dopants (M) in both materials being capable of substituting for Mn in MnO_6 to form MO_6.

Another interesting phenomenon of Fig. 2 is that [Ni]-OMS, and [Cu]-OMS decompose hydrogen peroxide faster than the rest of the materials. As mentioned previously, Langmuir adsorption isotherms were applied to study the reaction mechanism for H_2O_2 decomposition. One of our

primary considerations for the adsorption of H_2O_2 onto [M]-OMS materials involves the way in which the oxygen atoms of H_2O_2 attach to the coordination sites of MnO_6 where some oxygen ligands are missing. Here, oxygen atoms of H_2O_2 and coordination sites of MnO_6 without oxygen ligands function as Lewis base sites and Lewis acid sites, respectively. If this assumption is so, materials with a larger number of Lewis acid sites might provide a larger probability for adsorption of H_2O_2, therefore, yielding a faster rate for H_2O_2 decomposition. The reason why [Cu]-OMS material may have more of these types of sites might be due to Jahn–Teller distortion effects. As assumed previously, CuO_6 octahedra exist in the [Cu]-OMS system. Since Cu^{2+} has nine 3d electrons, according to the Jahn-Teller theorem, CuO_6 octahedra are not stable and must distort, leading to elongation of the z axis, as has been observed in a large number of Cu^{2+} complexes (17). Consequently, the magnitude of disorder in the [Cu]-OMS material may be enhanced. [Cu]-OMS materials are expected to have more lattice defects, corresponding to a larger number of Lewis acid sites.

It is still difficult to know how and why Ni^{2+} cations doped in the framework of [M]-OMS materials significantly increased the activity for H_2O_2 decomposition based on our data. However, previous research has shown that [M]-OMS materials with Ni dopants have greater acidity than other metal dopants (15, 16, 18). As assumed previously, the Lewis acid sites on [Ni]-OMS materials can react with the lone electron pairs on oxygen atoms of H_2O_2 and play a critical role for adsorption of H_2O_2 onto the surface of [Ni]-OMS materials. The adsorption may follow Langmuir adsorption isotherms for H_2O_2 decomposition over [Ni]-OMS materials. If Langmuir adsorption isotherms are followed, then in a certain range of Mn/Ni more Ni dopants in [Ni]-OMS materials will consequently result in more Lewis acid sites, which leads to a faster reaction rate for H_2O_2 decomposition.

B. Stability of Catalysts

The stability of these materials for H_2O_2 decomposition is another interesting phenomenon. Among all of the materials tested in our experiments, the structure of only [Fe]-OMS-1 material was changed to birnessite after reaction. Other catalysts still retained their original structures. This result suggests that the chemical stability of [M]-OMS materials for this reaction is good and might be related to the presence of transition metal dopants in their frameworks. For example, some dopants may diminish the stability of [M]-OMS materials, while others do not (18, 20). Additionally, the low activity of [Fe]-OMS-1 for H_2O_2 decomposition might be related to the change in structure and loss of the tunnels during H_2O_2 decomposition. In terms of stability in H_2O_2 decomposition, [M]-OMS-2 materials are more stable than [M]-OMS-1 materials.

C. Kinetic Studies

Table 2 shows that all supernatant solutions of H_2O_2 decomposition contain four types of cations, which include K^+, Mn^{2+}, Mg^{2+} and the corresponding transition metal dopants. The concentrations of these cation in the different supernatant solutions vary from one to another. Based on this fact, two possible mechanisms of H_2O_2 decomposition over [M]-OMS catalysts are possible. The reaction may be a heterogeneous or a combination of homogeneous and heterogeneous catalytic reactions (1–14). In order to investigate these two possible mechanisms, all of the supernatants were tested for H_2O_2 decomposition. Since the test results showed that these supernatants had no catalytic activity for H_2O_2 decomposition at 273 K, this result suggests that free cations released from [M]-OMS in aqueous H_2O_2 did not decompose H_2O_2 in these systems. Consequently, the H_2O_2 decomposition over [M]-OMS materials is considered to be a heterogeneous catalytic reaction. A possible mechanism for this decomposition over [M]-OMS catalysts is proposed from kinetic data as discussed below.

The kinetic studies of H_2O_2 decomposition over [M]-OMS materials were derived from the following process: first of all, H_2O_2 adsorbs at the active sites on the surface of [M]-OMS catalysts (21). Eventually, this is both an adsorption and an equilibrium step. This step is expressed by Eq. [5]:

$$H_2O_{2(aq)} + \text{[M]-OMS} \underset{k'}{\overset{k}{\rightleftarrows}} H_2O_2 \cdot \text{[M]-OMS}. \qquad [5]$$

Second, H_2O_2 adsorbing on [M]-OMS catalysts is activated by [M]-OMS catalysts and decomposed to water and atomic oxygen remaining on the surface of [M]-OMS materials. This step is illustrated by Eq. [6]

$$H_2O_2 \cdot \text{[M]-OMS} \rightarrow H_2O_{(aq)} + O \cdot \text{[M]-OMS}. \qquad [6]$$

Finally, oxygen atoms associated with [M]-OMS materials are then desorbed from [M]-OMS catalysts and combined to form gaseous oxygen. Since oxygen is only slightly soluble in water, gaseous oxygen immediately escapes from the aqueous solution. This step is described by Eq. [7]

$$2O \cdot \text{[M]-OMS} \rightarrow O_{2(g)} + 2\text{[M]-OMS}. \qquad [7]$$

Among the above three steps, the first one (Eq. [5]) is the key and rate-determining step, where the situation of adsorption is encountered and the Langmuir adsorption isotherm model is likely applicable. Regarding Eq. [5], we can consider H_2O_2 molecules in solution with a concentration of $[H_2O_2]$, which adsorb without dissociation onto a surface of [M]-OMS catalysts, and we can assume that the occupied fraction of sites on the surface of catalysts by H_2O_2 is $\theta_{H_2O_2}$. Since the rate of adsorption $dn_{H_2O_2}/dt$ is proportional to the rate of molecular collisions with unoccupied

sites, the adsorption rate expression is

$$\left(\frac{dn_{H_2O_2}}{dt}\right)ads = k(1-\theta_{H_2O_2})[H_2O_2]. \quad [8]$$

Because the rate of desorption should be proportional to the number of molecules adsorbed, the desorption rate expression can be expressed as

$$\left(\frac{dn_{H_2O_2}}{dt}\right)des = k'\theta_{H_2O_2.} \quad [9]$$

At equilibrium, the rate of adsorption equals the rate of desorption, so that Eq. [10] is

$$k(1-\theta_{H_2O_2})[H_2O_2] = k'\theta_{H_2O_2}. \quad [10]$$

The parameter $\theta_{H_2O_2}$is derived from Eq. [10]:

$$\theta_{H_2O_2} = \frac{k[H_2O_2]}{k'+k[H_2O_2]} = \frac{K_{H_2O_2}[H_2O_2]}{1+K_{H_2O_2}[H_2O_2]}. \quad [11]$$

In Eq. [11] $K_{H_2O_2} = k/k'$.

Here, $\theta_{H_2O_2}$ is the H_2O_2 surface coverage onto [M]-OMS materials and $K_{H_2O_2}$ is the equilibrium constant for Eq. [5], or the adsorption coefficient of the first step.

As mentioned above, for H_2O_2 decomposition over [M]-OMS materials, the reaction rate is taken to be proportional to the quantity of adsorbed H_2O_2 molecules on the surface of [M]-OMS materials. If an apparent first-order reaction is assumed for H_2O_2 decomposition over the [M]-OMS catalysts (22–28), the rate expression of the H_2O_2 decomposition over [M]-OMS materials can be simply written by the Langmuir–Hinshelwood kinetic model as shown in Eq. [12]:

$$-r_{H_2O_2} = k_{H_2O_2} \times \theta_{H_2O_2}. \quad [12]$$

Here, $r_{H_2O_2}$ is the rate of H_2O_2 decomposition on the surface of [M]-OMS catalysts, $k_{H_2O_2}$ is the rate constant and is independent of the H_2O_2 concentration. The parameter $\theta_{H_2O_2}$ is derived from the Langmuir adsorption isotherms as discussed previously. Equation [3] can then be derived from the combination of Eqs. [11] and [12].

$$-r_{H_2O_2} = k_{H_2O_2} \times \frac{K_{H_2O_2}[H_2O_2]_{(aq)}}{1+K_{H_2O_2}[H_2O_2]_{(aq)}}. \quad [13]$$

In Eq. [3] faster decomposition rates correspond to larger values of both $k_{H_2O_2}$ and $K_{H_2O_2}$, at least in theory.

Since the kinetic plots of H_2O_2 decomposition over [M]-OMS-2 in both Figs. 7 and 8 reveal a good linear relationship, the data from both Figs. 7 and 8 suggest that the Langmuir adsorption isotherm model might be suitable to the case discussed above. Therefore, the mechanism proposed here is possible and may fit H_2O_2 decomposition over [M]-OMS materials. The data in Table 1 show among all of the catalysts that the $k_{H_2O_2}$ values are very slightly different from each other, which suggests that different framework transition metal dopants and the amount of dopants do not affect the reaction pathway.

In Eq. [12] the $k_{H_2O_2}$ values for all of the [M]-OMS materials vary in a very small range. The apparent rate of reaction mainly depends on the surface coverage ($\theta_{H_2O_2}$) that should be proportional to the adsorption coefficient ($K_{H_2O_2}$) in the Langmuir adsorption isotherm model. Generally, faster reaction rates most likely correspond to larger values of $K_{H_2O_2}$. In Table 1, the decreasing order of magnitude of $K_{H_2O_2}$ for [M]-OMS-2 is exactly the same as the decreasing order of decomposition rate for [M]-OMS-2 as shown in both Figs. 2 and 3. For example, [Ni]-OMS-2 has the largest $K_{H_2O_2}$ and decomposes H_2O_2 most quickly. [Fe]-OMS-2 has the smallest $K_{H_2O_2}$ and decomposes H_2O_2 most slowly. [Cu]-OMS-2 has a larger $K_{H_2O_2}$ than [Fe]-OMS-2 and decomposes H_2O_2 faster than [Fe]-OMS-2. The results here support the suggestion that the effect of different framework transition metal dopants in [M]-OMS materials may not be strong enough to change the reaction pathway of H_2O_2 decomposition over [M]-OMS materials, but they may play an important role in changing the rate of the reaction.

It is worthwhile to understand how transition metal dopants in the framework of [M]-OMS-2 materials affect their adsorption coefficients ($K_{H_2O_2}$). Adsorption is basically classified into two categories, i.e., chemical and physical adsorptions. Physical adsorption is caused by van der Waals attractive forces such as dipole–dipole interaction and induced dipoles and is similar in character to condensation of vapor molecules onto the liquid of the same composition. Chemical adsorption involves chemical bonding and is similar in character to a chemical reaction like an acid–base reaction and also may involve the transfer of electrons between adsorbent and adsorbate. However, borderline cases can also exist (29).

Regarding H_2O_2 decomposition over [M]-OMS materials, Lewis acid sites are mainly caused by vacancies of oxygen atoms located at vertices of octahedral structural units of [M]-OMS materials (15–16). Lewis base sites are due to lone electron pairs on oxygen atoms of H_2O_2. Chemical adsorption can readily occur due to acid–base type reactions. For H_2O_2 adsorbed onto [M]-OMS materials, the adsorption is thought to be attributed mainly to chemical adsorption. On examining the electronic configurations of Fe^{3+}, Ni^{2+}, and Cu^{2+}, it is easy to see that each cation has five, eight, or nine 3d electrons, respectively. Based on crystal field theory, in these metal–oxygen octahedral complexes, a central metal cation like Fe^{3+} with fewer electrons in the 3d orbitals may have more 3d orbitals available for interaction with oxygen ligands. Therefore, interactions between the central metal and oxygen ligands may be stronger, so the probability of missing oxygen ligands is reduced.

The consequences of this effect may result in the reduction of Lewis acid sites followed by a diminishing of chemical adsorption. In other cases of central metal cations like Ni^{2+} or Cu^{2+} with more 3d electrons, the situation may be reversed. Assumptions about H_2O_2 decomposition are as follows: (1) the adsorption of H_2O_2 onto [M]-OMS materials might be due to chemical adsorption. (2) Lewis acid sites in [M]-OMS materials are responsible for the chemical adsorption. (3) Increasing the number of Lewis acid sites onto [M]-OMS materials may result from the introduction of the first-row transition metal cations with a large number of 3d electrons. (4) A larger number of Lewis acid sites corresponds to more transition metal cations with more 3d electrons in the framework of the [M]-OMS materials. The data obtained from this research are consistent with the above assumptions.

V. CONCLUSIONS

The following conclusions have been revealed in this work:

(1) Most [M]-OMS materials decompose H_2O_2 faster than commercial MnO_2; [M]-OMS-2 materials do so even faster than [M]-OMS-1 materials.

(2) Different transition metal dopants in the framework of [M]-OMS materials vary the activities of these materials for H_2O_2 decomposition. Ni dopants significantly enhance the catalytic activity of both [M]-OMS materials for H_2O_2 decomposition. [Ni]-OMS-2 gives higher catalytic activity than others for H_2O_2 decomposition.

(3) Quantitative effects of transition metal dopants in the framework of [M]-OMS are also effective factors for controlling catalytic activity of [M]-OMS materials. Regarding [Ni]-OMS-2, a higher ratio of Ni/Mn gives a higher catalytic activity for H_2O_2 decomposition.

(4) In terms of H_2O_2 decomposition, [M]-OMS-2 materials are more stable than [M]-OMS-1 materials.

(5) The mechanism of H_2O_2 decomposition over [M]-OMS materials may follow the Langmuir–Hinshelwood kinetic model. Regarding Langmuir adsorption isotherms, the adsorption of H_2O_2 on [M]-OMS materials might be dominated by chemical adsorption that may be mainly attributed to Lewis acid sites existing on [M]-OMS materials.

ACKNOWLEDGMENTS

We thank the U.S. Department of Energy, Office of Basic Energy Sciences, Division of Chemical Sciences, and Texaco, Inc. for support of this research.

REFERENCES

1. Abbot, J., and Brown, D. G., *Can. J. Chem.* **68**, 1537 (1990).
2. Youssef, N. S., Kamel, E. S., and Selim, M. M., *Bull. Soc. Chim. Fr.* **12**, 648 (1991).
3. Salem, I. A., Salem, M. A., and Gemeay, A. H., *J. Mol. Catal.* **84**, 67 (1993).
4. Onuchukwu , A. I., *J. Chem. Soc. Faraday Trans.* **1**, 1447 (1984).
5. Mucka, V., *Collection Czechoslovak Chem. Commun.* **51**, 1874 (1986).
6. Mucka, V. C., *J. Coll. Czechoslov. Chem. Commun.* **40**, 236 (1975).
7. Mucka, V., *J. Phys. Chem.* **78**, 1653 (1974).
8. Kolesnikova, I. P., and Voloshin, A.G., *Kinet. i Katal.* **27**, 1245 (1986).
9. Kanungo, S. B., Parida, K. M., and Sant, B. R., *Electrochem. Acta.* **26**, 1157 (1981).
10. El-Wakil, A. M., Mostafa, M. R., El-Tagoury, M. M., Mohammad, F. S., and Hassan, S. M., *Pak. J. Aci. Ind. Res.* **32**, 306 (1989).
11. Arutyunyan, A. Z., Grigoryan, G. L., and Nalbandyan, A. B., *Kinet. i Katal.* **28**, 969 (1987).
12. Arutyunyan, A. Z., Grigoryan, G. L., and Nalbandyan, A. B., *Kinet. i Katal.* **27**, 1352 (1986).
13. Arutyunyan, A. Z., Grigoryan, G. L., and Nalbandyan, A. B., *Kinet. i Katal.* **26**, 785 (1985).
14. Ahuja, L. D., Rajeshwer, D., and Nagpal, K. C., *J. Colloid. & Interface Sci.* **119**, 481 (1987).
15. Shen, Y. F., Zerger, R. P., DeGuzman, R. N., Suib, S. L., McCurdy, L., Potter, D. l., and O'Young, C. L., *Science* **260**, 511 (1993).
16. De Guzman, R. N., M.S. thesis, University of Connecticut, 1994.
17. Cotton, F. A., Wilkinson, G., and Gaus, P. L., (Eds.), "*Basic Inorganic Chemistry*," 2nd ed., p. 466. Wiley, New York, 1987.
18. Shen, Y. F., Suib, S. L., and O'Young, C. L., *J. Am. Chem. Soc.* **116**, 11020 (1994).
19. Oelfke, W. C., *J. Chem. Phys.* **51**, 5336 (1969).
20. Yin, Y. G., Xu , W. Q., DeGuzmans, R., Suib, S. L., and O'Young, C. L., *Inorg. Chem.* **33**, 4384 (1994).
21. Ram, R. N., *Kinet. Katal.* **25**, 1105 (1984).
22. Costisor, O., Policer, S., and Mracer, M., *Chem. Bull. Tech. Univ. Timisoara* **37**, 31 (1992).
23. Dimitrova, V., Manev, S., Kirova, T., Mitov, M., and Lazarov, D., *God. Sofii. Univ., "Sv. Kliment Okhridski," Khim. Fak.* **86**, 137 (1993).
24. Miller, C. M., and Valentine, R. L., *Chem. Oxid.* **3**, 80 (1993).
25. Salem, I. A., *Int. J. Chem. Kinet.* **26**, 341 (1994).
26. Salem, I. A., *J. Mol. Catal.* **87**, 25 (1994).
27. Shpota, G. P., and Tarkovskaya, I. A., *Katal. i Katal.* **20**, 69 (1982).
28. Schwab, G. M., and Mucka, V. Z., *Phys. Chem.* **93**, 77 (1974).
29. Satterfield, C. N., "Heterogeneous Catalysis in Principle," 1st ed., p. 35. New York, McGraw–Hill, 1980.